

Interaction between plasma and electromagnetic field in ion source of 10 cm ECR ion thruster

Hao Mou(牟浩), Yi-Zhou Jin(金逸舟), Juan Yang(杨涓), Xu Xia(夏旭), and Yu-Liang Fu(付瑜亮)
Citation: Chin. Phys. B, 2022, 31 (**7**): 075202. DOI: 10.1088/1674-1056/ac4906
Journal homepage: http://cpb.iphy.ac.cn; http://iopscience.iop.org/cpb

What follows is a list of articles you may be interested in

Numerical investigation of radio-frequency negative hydrogen ion sources by a three-dimensional fluid model

Ying-Jie Wang(王英杰), Jia-Wei Huang(黄佳伟), Quan-Zhi Zhang(张权治), Yu-Ru Zhang(张钰如), Fei Gao(高飞), and You-Nian Wang(王友年)
Chin. Phys. B, 2021, 30 (**9**): 095205. DOI: 10.1088/1674-1056/ac0e21

Analysis of extreme ultraviolet spectral profiles of laser-produced Cr plasmas

L Wu(吴磊), M G Su(苏茂根), Q Min(敏琦), S Q Cao(曹世权), S Q He(何思奇), D X Sun(孙对兄), C Z Dong(董晨钟)
Chin. Phys. B, 2019, 28 (**7**): 075201. DOI: 10.1088/1674-1056/28/7/075201

Practical 2.45-GHz microwave-driven Cs-free H^- ion source developed at Peking University

Tao Zhang(张滔), Shi-Xiang Peng(彭士香), Wen-Bin Wu(武文斌), Hai-Tao Ren(任海涛), Jing-Feng Zhang(张景丰), Jia-Mei Wen(温佳美), Teng-Hao Ma(马腾昊), Yao-Xiang Jiang(蒋耀湘), Jiang Sun(孙江), Zhi-Yu Guo(郭之虞), Jia-Er Chen(陈佳洱)
Chin. Phys. B, 2018, 27 (**10**): 105208. DOI: 10.1088/1674-1056/27/10/105208

A miniaturized 2.45 GHz ECR ion source at Peking University

Jia-Mei Wen(温佳美), Shi-Xiang Peng(彭士香), Hai-Tao Ren(任海涛), Tao Zhang(张滔), Jing-Feng Zhang(张景丰), Wen-Bin Wu(武文斌), Jiang Sun(孙江), Zhi-Yu Guo(郭之虞), Jia-Er Chen(陈佳洱)
Chin. Phys. B, 2018, 27 (**5**): 055204. DOI: 10.1088/1674-1056/27/5/055204

Understanding hydrogen plasma processes based on the diagnostic results of 2.45 GHz ECRIS at Peking University

Wen-Bin Wu(武文斌), Hai-Tao Ren(任海涛), Shi-Xiang Peng(彭士香), Yuan Xu(徐源), Jia-Mei Wen(温佳美), Jiang Sun(孙江), Ai-Lin Zhang(张艾霖), Tao Zhang(张滔), Jing-Feng Zhang(张景丰), Jia-Er Chen(陈佳洱)
Chin. Phys. B, 2017, 26 (**9**): 095204. DOI: 10.1088/1674-1056/26/9/095204

Interaction between plasma and electromagnetic field in ion source of 10 cm ECR ion thruster

Hao Mou(牟浩)[1], Yi-Zhou Jin(金逸舟)[2], Juan Yang(杨涓)[1,†], Xu Xia(夏旭)[1], and Yu-Liang Fu(付瑜亮)[1]

[1] *College of Astronautics, Northwestern Polytechnical University, Xi'an* 710072, *China*
[2] *Shanghai Institute of Space Electric Propulsion, Shanghai* 200000, *China*

(Received 5 October 2021; revised manuscript received 2 January 2022; accepted manuscript online 7 January 2022)

Through diagnosing the plasma density and calculating the intensity of microwave electric field, four 10 cm electron cyclotron resonance (ECR) ion sources with different magnetic field structures are studied to reveal the inside interaction between the plasma, magnetic field and microwave electric field. From the diagnosing result it can be found that the plasma density distribution is controlled by the plasma generation and electron loss volumes associated with the magnetic field and microwave power level. Based on the cold plasma hypothesis and diagnosing result, the microwave electric field intensity distribution in the plasma is calculated. The result shows that the plasma will significantly change the distribution of the microwave electric field intensity to form a bow shape. From the boundary region of the shape to the center, the electric field intensity varies from higher to lower and the diagnosed density inversely changes. If the bow and its inside lower electric field intensity region are close to the screen grid, the performance of ion beam extracting will be better. The study can provide useful information for the creating of 10 cm ECR ion source and understanding its mechanism.

Keywords: electron cyclotron resonance plasma, plasma diagnosing, ion source

PACS: 52.75.Di, 52.70.–m, 52.75.–d **DOI:** 10.1088/1674-1056/ac4906

1. Introduction

The 10 cm ECR ion thruster (ECRIT) has the properties of long-life span, high reliability and high specific impulse. The properties make it a candidate for the application in space flying missions.[1–3]

The 10 cm ECRIT is composed of the ECR ion source and neutralizer, both of which ionize the propellant gas according to the ECR heating mechanism. This kind of thruster can regulate the thrust through changing the microwave power, mass flow rate and acceleration voltage. Nowadays, the commercial market of spacecraft in low Earth orbit (LEO) is fast growing, it is required to perform the maneuvers including attitude control, drag compensation, and evenly to fuel the electric thruster with the rare gas at the flying orbit.[4,5] The new space flying mission needs to study the performance of ECRIT operating at the rare atmosphere environment,[6] in which N_2 is a main component and its ionization takes an important role in the rare gas discharge. The first ionization energy threshold of N_2 is similar to that of argon.[7,8] Therefore, studying the plasma property of 10 cm ECRIT operating on argon gas can provide useful information to understand the gas ionization and performance property as the thruster running at rare atmosphere environment.

In previous study,[9] four kinds of ECR ion source of 10 cm ECRIT operating on argon were developed to experimentally study the influence of magnetic field on ion beam extracting performance. Define the energy absorbing efficiency of ion source as η, which is the ratio of the absorbed to incident microwave power. The state of ion source with low, medial and high exhausted ion beam current is defined separately at low, medial and high level. It was found that the different sources can operate on different states as the incidence microwave power and η changing.

Coral *et al.*[10] studied the local electron behavior in an ECR discharge using the estimation method, based on measured performance parameter and Langmuir probe diagnostics to evaluate the microwave power absorption efficiency and clarify the physics behind the performance variations. Tani *et al.*[11] designed and tested a new ECR ion source using a 10 cm ECRIT. They found that the performance of the new source was improved and the plasma production volume enlarged. However, this improved performance comes with an increase in the electric power consumption.

Even the above references presented the influence of magnetic field on the ion beam performance and developed a new design for improved performance at increasing power consumption, it is still required to research the interaction between the plasma, magnetic field and microwave electric field inside of the 10 cm ECR ion source. This is because the high density of plasma upwind of the screen grid will generate a high ion beam current and best thrust performance, the plasma density upwind the grid is also decided by its whole distribution inside of the ECR ion source. For ECR ion source, the plasma density distribution is decided by the electron behav-

[†]Corresponding author. E-mail: yangjuan@nwpu.edu.cn

© 2022 Chinese Physical Society and IOP Publishing Ltd

ior of migrating to the system wall and resonating with the microwave electric field on ECR layer. This behavior is associated with the magnetic field structure and interfered with the microwave electric field intensity.[12–14] Therefore, reviewing the multi-field interaction of 10 cm ECR ion source running on argon gas is required as creating the source and explaining its mechanism. It is necessary to use the probe diagnosing method to make clear the plasma density distribution and its relation with magnetic field.

The microwave electric field intensity in an ECR ion source had ever been firstly detected via EO probe.[15] Another method to obtain the microwave electric field intensity in plasma is PIC method combined by FDTD, however, using this method is time consuming and the microwave power absorbed by plasma is required modified for much more times through varying the microwave electric field intensity to obtain the appropriate result.[16] Through the software of COMSOL and based on the diagnosed plasma density distribution, calculating the microwave electric field intensity in the plasma of ECR ion source is convenient to make clear the relationship of plasma density and microwave electric field intensity. Therefore, through calculating the plasma dielectric tensor based on the diagnosed plasma density,[17] the microwave electric field intensity in plasma can be simulated more actually. This method is time saving.

Based on the above background, in this study, four 10 cm ECR ion sources with different magnetic field properties are generated to reveal the multi-field interaction of ECR ion source. In Section 2, the four ion sources with different magnetic field structures, plasma density diagnosing system and the methods for diagnosing and calculation are described. In Section 3, the result and analysis of the diagnosing and calculation and the revelation obtained from the study are presented. Section 4 is the conclusion.

2. The 10 cm ECR ion source and study methods

2.1. The 10 cm ECR ion source

As shown by Fig. 1, the 10 cm ECR ion source is composed of a cylindrical waveguide, a tapered resonant cavity made by magnetic yoke, two magnet rings made by samarium cobalt, gas distributor, probe antenna to transmit microwave into the source, screen and acceleration grids. Microwave at the frequency of 4.2 GHz is coupled into the ion source through the probe antenna. Gas is put into the ion source through the gas distributor at the exit of the cylindrical waveguide. Two magnet rings are assembled on the inner surface of the tapered resonant cavity. When the gas and the microwave energy are put into the source, the plasma will be generated under the magnetic field formed by the magnet rings and yoke. In the plasma, extraordinary (X), right and left hand circularly polarized (R and L) waves exist.[18,19] As microwave frequency is equal to that of the electron gyrating, $\omega = \omega_{ce}$, R wave will become the ECR wave to heat electron, and cut off as $\omega_{ce} < \omega < \omega_R$, where $\omega_R = \frac{\omega_{ce}}{2} + \sqrt{\omega_{pe}^2 + \frac{\omega_{ce}^2}{4}}$. As $\omega^2 = \omega_{ce}^2 + \omega_{pe}^2$, X wave will become upper hybrid resonant (UHR) wave to heat electrons, and cut off as $\omega_R < \omega < \omega_L$, where $\omega_L = -\frac{\omega_{ce}}{2} + \sqrt{\omega_{pe}^2 + \frac{\omega_{ce}^2}{4}}$. L wave will cut off as $\omega > \omega_L$. Therefore, the ECR and UHR waves are associated with the procedure of electron heating and plasma generation. However, UHR wave frequency, $\omega^2 = \omega_{ce}^2 + \omega_{pe}^2$, is decided by plasm self-consistent oscillation and electron gyrating around magnetic flux line, therefore this wave energy to heat electron is related with magnetic flux density and plasma density. Compared with UHR wave, the ECR layer is obviously important for plasma generation[18] and used to define the magnetic field of ECR ion source to three regions. Closed magnetic mirror crosses the ECR layer, through which electrons pass multiple times to gain microwave energy at each passage, and this mirror composes the region 1 and presents plasma generation volume. Closed magnetic mirror not crossing the ECR layer and heating electrons forms the region 2. Two opened magnetic mirrors crossing the ECR layer, on which electron can gain energy two times before being lost to the system walls, compose the two regions of 3(a) and 3(b), and electron loss volumes.

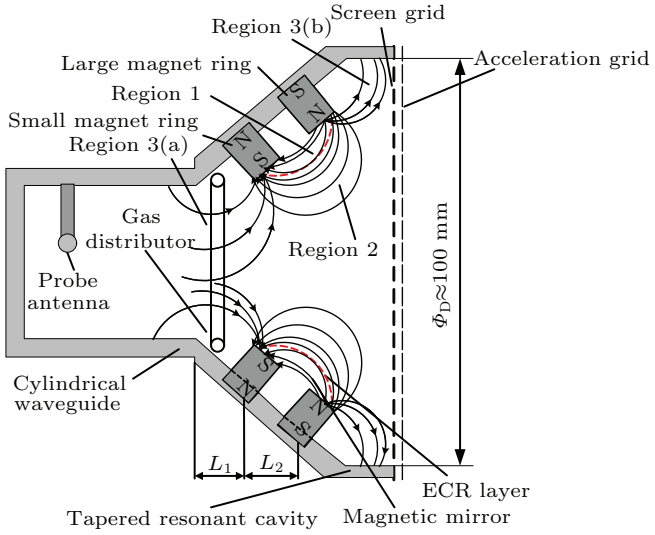


Fig. 1. Schematics of ECR ion source.

As Fig. 2 showed, at the fixed length, L, between the surfaces A and B, four ion sources, numbered from 1 to 4, with different magnetic field structures and ECR layers are formed according to the lengths of L_1 and L_2, which separately present the distance between the small magnetic ring and surface A, the large and small magnetic ring centers. The distribution of magnetic flux density in the sources was calculated through the COMSOL. The vacuum, magnetic yoke and permanent magnet of samarium cobalt separately with relative permeability in

1, 4000 and 1.36 were considered in calculation. The calculation result was calibrated through the measuring data. As the microwave frequency used by the ion source is 4.2 GHz, the magnetic flux density on ECR layer is 0.15 T. The structure property of the four sources is showed in Table 1. The different volumes of regions 1, 3(a) and 3(b) provide the condition to study the volume influence on plasma distribution and indicate the multi-field interaction inside of ion source.

Table 1. Structure property of four ion sources.

Source	Structure property
1	Largest region 1, most beneficial for heating. Larger region 3(a), higher loss. Smallest region 3(b), least loss.
2	Larger region 1, more beneficial for heating. Smallest region 3(a), least loss. Smaller region 3(b), lower loss.
3	Smaller region 1, lower beneficial for heating. Largest region 3(a), highest loss. Larger region 3(b), higher loss.
4	Smallest region 1, least beneficial for heating. Smallest region 3(a), least loss. Largest region 3(b), highest loss.

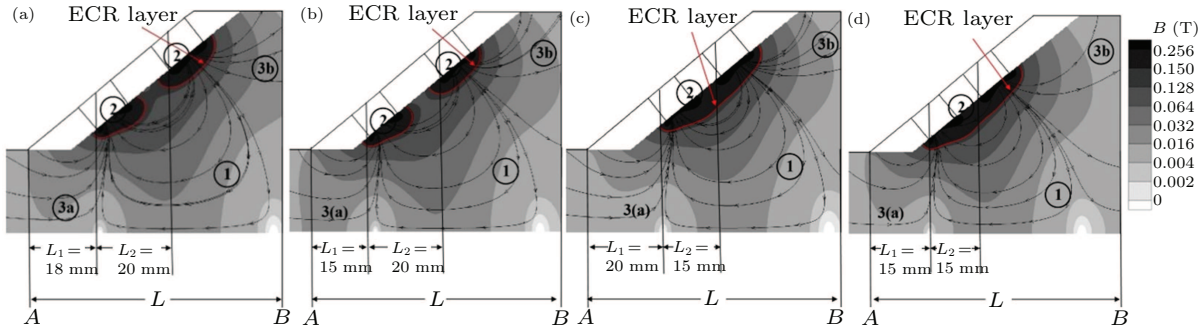


Fig. 2. Simulated magnetic flux density in (a) source 1, (b) source 2, (c) source 3, (d) source 4.

2.2. Study methods

2.2.1. Diagnosing system and method

Diagnosing the plasma density inside of the four ECR ion sources will provide important information to analyze the relation between the plasma density and magnetic fields, and also help to understand the ECR and UHR heating property.

The diagnosing system is showed by Fig. 3(a). The diagnosing system is composed of solid state microwave source, circulator, attenuator, power meter, ECR ion source, a bent Langmuir probe, 2D coordinator, electric power source, computer, gas tank and controller, vacuum chamber and oil diffusion vacuum pump. The incident microwave power of the ion source is calibrated before the experiment, and the reflected microwave power from the ECR ion source is transmitted to the power meter for measurement. The precision of 2D coordinator, power meter for microwave power measuring, the ammeter and voltmeter used to measure the current and voltage of the probe are separately within 0.5 mm/100 mm, 0.1 W/100 W, and 0.1%. For diagnosing, as shown by Fig. 3(b), only one punched screen grid for passing probe is used. Under the action of the 2D coordinator, the Langmuir probe can be moved step-by-step in the radial and axial direction of diagnosing plane, XOZ. The data acquisition line is used to transfer the collected current and voltage signals of probe to a computer for analyzing the plasma density. The tip axis of bent Langmuir probe is vertical to the diagnosis plane, its diameter and length related with current collecting is separately 0.2 mm and 5 mm.

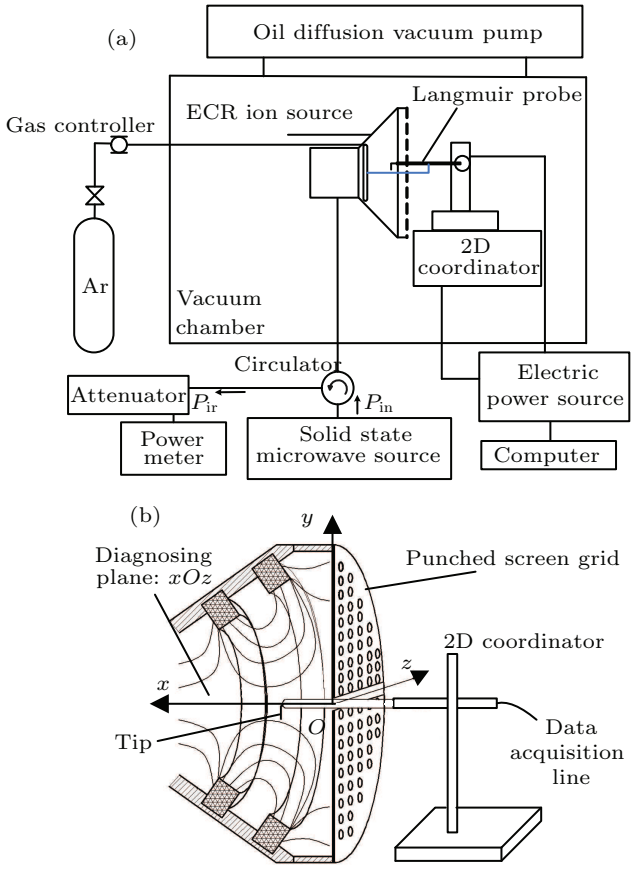


Fig. 3. Plasma diagnosing system: (a) facility, (b) diagnosing plane coordinate.

In the experiment, when the plasma was generated in ion source, before the probe is inserted into the ion source, the reflected power of the four sources is generally less than 20% of

incident power. After the probe is inserted into, the reflected power fluctuates 5% on the basis of 20%. And since the ion source and the screen grid are grounded, the grid current is always zero during the diagnosing procedure.

The electron density diagnosing is decided by the relation between the electron and ion cyclotron, and probe tip radius, r_e, r_i and r_p. In the ion source running on argon, the cyclotron radius of electron and ion, r_e and r_i, are estimated to be 0.025 and 2.2 mm, respectively. Compared with the tip radius, we have $r_p = 0.1$ mm, $r_e < r_p < r_i$. Therefore, the magnetic field influences the electron saturation current due to the electron cyclotron, however, hardly influences the ion saturation current. Hence for the ECR ion source, according to the orbital motion limit (OML) model, the ion density can be obtained by $n_i = \frac{\pi^2}{2A_p^2 e^2}\frac{M}{|e|}\frac{\mathrm{d}I_i^2}{\mathrm{d}|V|}$, where M, I_i and A_p are ion mass, the collected current in the ion saturation region and the surface area of the probe, respectively. According to the quasi-neutrality property of plasma, the diagnosed ion density, n_i, is used as plasma density.

In the diagnosing experiment, the thin tip can decrease the magnetic field interference on the collecting current and increase the special resolution of experiment.[20–22] The length between the adjacent diagnosing points is 5 mm, which is larger than the thickness of sheath and ensures the accuracy of data acquisition. The diagnosing experiment is just at three microwave power levels of 10 W, 20 W and 30 W, while the argon gas flow rate is fixed at 4 sccm.

2.2.2. Calculation method

Calculating the electric field intensity distribution of the microwave in ECR plasma will provide some important information to analyze the relation between the microwave electric field intensity and plasma density. According to the electrodynamics,[23] the density of microwave energy is $\frac{1}{2}\varepsilon \boldsymbol{E}^2 + \frac{1}{2}\mu \boldsymbol{H}^2$, in which only the part of $\frac{1}{2}\varepsilon \boldsymbol{E}^2$ can be used to heat the electron due to the weakest Lorentz force on electron. From the principle of microwave, $\boldsymbol{E}_{\max}^2$ is proportional to the wave power, where $\boldsymbol{E}_{\max}$ is the amplitude of microwave electric field intensity and increases with microwave power. This property of microwave demonstrates that the microwave electric field intensity distribution is independent of the microwave power, but its value varies with the power.

Based on the cold plasma hypothesis and in Cartesian coordinate system, according to the electron moving, current density and Maxwell equations, the wave transmission in plasma can be described as

$$\nabla \times \nabla \times \boldsymbol{E} - \omega^2 \mu_0 \varepsilon \boldsymbol{E} = 0, \tag{1}$$

$$\varepsilon = \varepsilon_0 \begin{bmatrix} 1 - \mathrm{j}\dfrac{\omega_p^2}{\omega}\dfrac{\omega_x^2 + (\nu + \mathrm{j}\omega)^2}{\Delta} & -\mathrm{j}\dfrac{\omega_p^2}{\omega}\dfrac{\omega_x\omega_y - (\nu+\mathrm{j}\omega)\omega_z}{\Delta} & -\mathrm{j}\dfrac{\omega_p^2}{\omega}\dfrac{\omega_x\omega_z + \omega_z(\nu+\mathrm{j}\omega)}{\Delta} \\ -\mathrm{j}\dfrac{\omega_p^2}{\omega}\dfrac{\omega_x\omega_y + \omega_z(\nu+\mathrm{j}\omega)}{\Delta} & 1 - \mathrm{j}\dfrac{\omega_p^2}{\omega}\dfrac{\omega_y^2 + (\nu+\mathrm{j}\omega)^2}{\Delta} & -\mathrm{j}\dfrac{\omega_p^2}{\omega}\dfrac{\omega_y\omega_z - \omega_x(\nu+\mathrm{j}\omega)}{\Delta} \\ -\mathrm{j}\dfrac{\omega_p^2}{\omega}\dfrac{\omega_x\omega_z - \omega_y(\nu+\mathrm{j}\omega)}{\Delta} & -\mathrm{j}\dfrac{\omega_p^2}{\omega}\dfrac{\omega_y\omega_z + \omega_x(\nu+\mathrm{j}\omega)}{\Delta} & 1 - \mathrm{j}\dfrac{\omega_p^2}{\omega}\dfrac{\omega_z^2 + (\nu+\mathrm{j}\omega)^2}{\Delta} \end{bmatrix}, \tag{2}$$

where $\boldsymbol{E}$, ε, ε_0 and μ_0 are separately the complex number of microwave electric field intensity, the relative permittivity tensor, vacuum permittivity and permeability tensor. In the permittivity tensor,

$$\Delta = \left(\nu + \mathrm{j}\omega_p\right)^3 + \left(\nu + \mathrm{j}\omega_p\right)\left(\omega_x^2 + \omega_y^2 + \omega_z^2\right), \tag{3}$$

$$\omega_p = \sqrt{\frac{ne^2}{\varepsilon_0 m_e}}, \tag{4}$$

$$\omega_i = eB_i/m_e, \quad i = x, y, z, \tag{5}$$

where m_e, e, j and ν are separately electron mass, electronic charge quantity, imaginary unit and electron collision frequency. Equation (1) and formula (2), without the influence of wave power, build the relationship between the plasma density, magnetic field and microwave electric field, and the wave transmission and electric field intensity distribution are not associated with power but related with plasma density, n. After calculating the permittivity tensor and presenting plasma density, n, by diagnosed parameter, n_i, the complex number module value of microwave electric field intensity can be obtained by solving Eq. (1) with COMSOL software.

3. Result and analysis

3.1. Result of diagnosing and analysis on the interaction between magnetic field and plasma density

The spatial distributions of the diagnosed plasma density at each ion source configuration, power levels of 10 W, 20 W and 30 W and fixed argon gas flow rate of 4 sccm are shown in Fig. 4, where the red and green lines present the ECR and UHR layer, respectively. The electrons on the whole ECR layer can resonate with microwave electric field and be heated. However, on the UHR layer, only the small blue circle region, where the electron oscillating and resonating frequencies satisfy the relation of $\omega^2 = \omega_{ce}^2 + \omega_{pe}^2$, can provide the condition for electron heating. Therefore, in the ion source, electron heating mainly happens on the ECR layer, and the region of

UHR wave acting on electron is so small to be neglected. The diagnosing result shows that the diagnosed density distribution of the four sources forms a bow shape expanding towards screen grid as power increasing. From the boundary of bow shape to the center, the density varies from lower to higher.

At the power level of 10 W, the plasma areas of the sources position all in region 1. The whole plasma area in source 1 is less than source 2. In sources 3 and 4, the whole ion density regions are smaller than sources 1 and 2. Therefore, only in source 2 the plasma density upwind the screen grid is the highest. As the microwave power is increased to 20 W, the ion density of the all sources increases largely, also the whole density region in sources 4, 3, 1, and 2 is from smaller to larger, and the variation of density before the screen grid is from lower to higher in the same serial number. This situation also presents that only in source 2 the plasma density upwind the screen grid is the highest. When the microwave power continues increasing to 30 W, the diagnosed density of the all sources increases further, the high density and whole plasma region in sources 4, 3, 2, and 1 is from smaller to larger. Compared with other sources, the plasma area of the source 1 enlarges mostly in all directions to generate higher plasma density distribution upwind the screen.

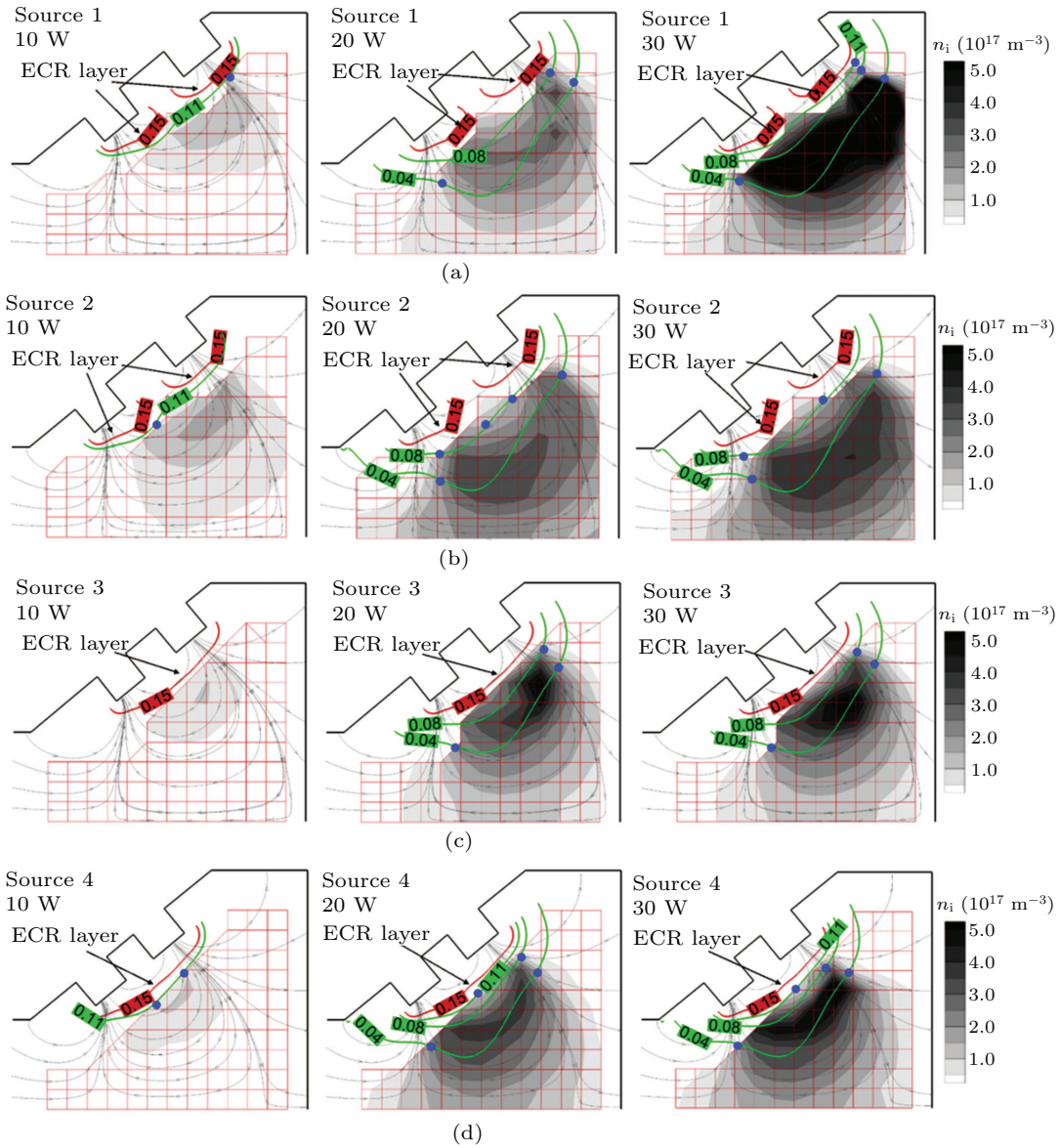


Fig. 4. Diagnosed density in source (a) 1, (b) 2, (c) 3 and (d) 4 at fixed gas flow rate of 4 sccm and power levels of 10 W, 20 W and 30 W. The lines of 0.15, 0.11, 0.8 and 0.4 respectively represent the magnetic flux density in their area, and the unit is T.

From the plasma diagnosing results, it can be seen the density distribution is decided by not only the power level but also the magnetic field. At the low and medial power level of 10 W and 20 W, the electron loss controls the plasma distribution, because at the two power levels few motive electrons can be generated to ionize gas. As Table 1 showed, even the volumes of regions 1 and 3(a) in source 1 are larger than those of source 2, and the volume of region 3(b) is inversely smaller

compared with source 2, the electron annihilation caused by the longer range of migrating in region 1 is faster than that of source 2, and consequently the whole plasma region and density upwind the screen grid of source 1 is smaller and lower compared with source 2. Compared with source 4, the regions 1 and 3(b) of source 3 are separately larger and smaller to generate a larger plasma region and higher density area upwind the screen grid. Compared with sources 1 and 2, in source 3 the smaller region 1, larger regions 3(a) and (b) make the lower density distribution upwind the screen grid.

At the power level of 30 W, much more wave energy heats electrons to increase density, the electron loss is much lower compared with plasma generation. For the four sources, the source 1 has the largest region 1 and smallest region 3(b), even the electron loss in region 3(a) with larger volume is higher, the gas ionization at high power compensates the loss, therefore the whole plasma area and density upwind screen grid will be the largest and highest, separately. As for sources 2, 3 and 4, the region 1 of source 2 is the largest, and its plasma density distribution property is similar to that of source 1. This situation explains that at high power level the plasma generation volume decides the plasma distribution.

3.2. Result of calculation and analysis on the interaction between plasma density and microwave electric field

To prevent the huge data operation, the calculating parameter is chosen as $\log_{10}(|\boldsymbol{E}|+1)$, where $|\boldsymbol{E}|$ is the complex number modulus of the microwave electric field intensity. For verifying the influence of microwave power on the electric field intensity, the source 4 with inside empty environment and filled by plasma generated at microwave power of 30 W is calculated at the transmission microwave powers of 10 W, 20 W and 30 W. The result is showed by Fig. 5, which demonstrates that the power levels influence the magnitudes of calculated parameter, however hardly change their distributions in empty and plasma environments separately. It is the plasma density to vary the calculation result largely. Therefore, the microwave electric field intensity in the four sources is calculated only at one power level of 30 W for wave transmission and three power levels of 10 W, 20 W and 30 W for plasms generation or diagnosed plasma density. The results are shown by Fig. 6.

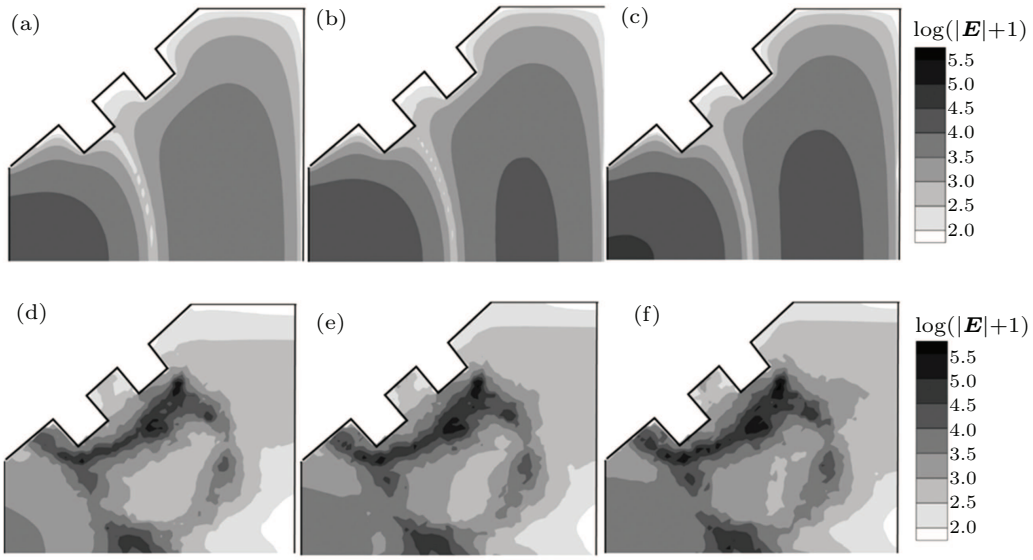


Fig. 5. The distribution of calculated parameter in source 4 without plasma and at microwave power of (a) 10 W, (b) 20 W, (c) 30 W, and with plasm induced by power of 30 W and at microwave power of (d) 10 W, (e) 20 W, (f) 30 W.

Before the plasma is generated, it can be seen from Fig. 6 that $\log_{10}(|\boldsymbol{E}|+1)$ distributions in all the sources are similar and relatively uniform, and the maximum calculated parameter is also around the axis line, which shows that the wave can transmit to the whole cavity space. But when the plasma is generated at power level of 10 W, as showed by the related pictures of Fig. 6, the calculated parameter is non-uniform, and concentrates around ECR layers, where the diagnosed density is conversely much lower as Fig. 4 showing.

When the power to generate plasma increases from 10 W to 30 W, in the four sources the regions of the highest calculated parameter gradually form bow shapes similar to those of density distribution. The two kinds of bow shape overlap as showed by Figs. 4 and 6. The calculated values inside of boundary regions are higher than those in the center areas, however the density distributions in the bow shapes of Fig. 4 present reverse variations. The calculated parameter and plasma density distributions imply that the plasma has the property of dissipative medium, the large area of higher density plasma obtain more wave energy to form the large region of the low microwave electric field intensity.

As the four sources filled with plasma generated at the power of 10 W, compared with sources 1, 3 and 4, in source

2 the calculated parameter and the plasma density before the screen grid is separately weakest and highest as Figs. 4 and 6 showed. When the plasma is induced at the power of 20 W and 30 W, compared with sources 3 and 4, in sources 1 and 2 the weakest microwave electric field intensity range is very near to the screen grid, and it is reasonable to observe the higher density distribution before the screen grid. In this point of view, it demonstrates that if the plasma density bow and the lower electric field intensity region inside of its bow are near to the screen grid, the density upwind the screen grid will be higher.

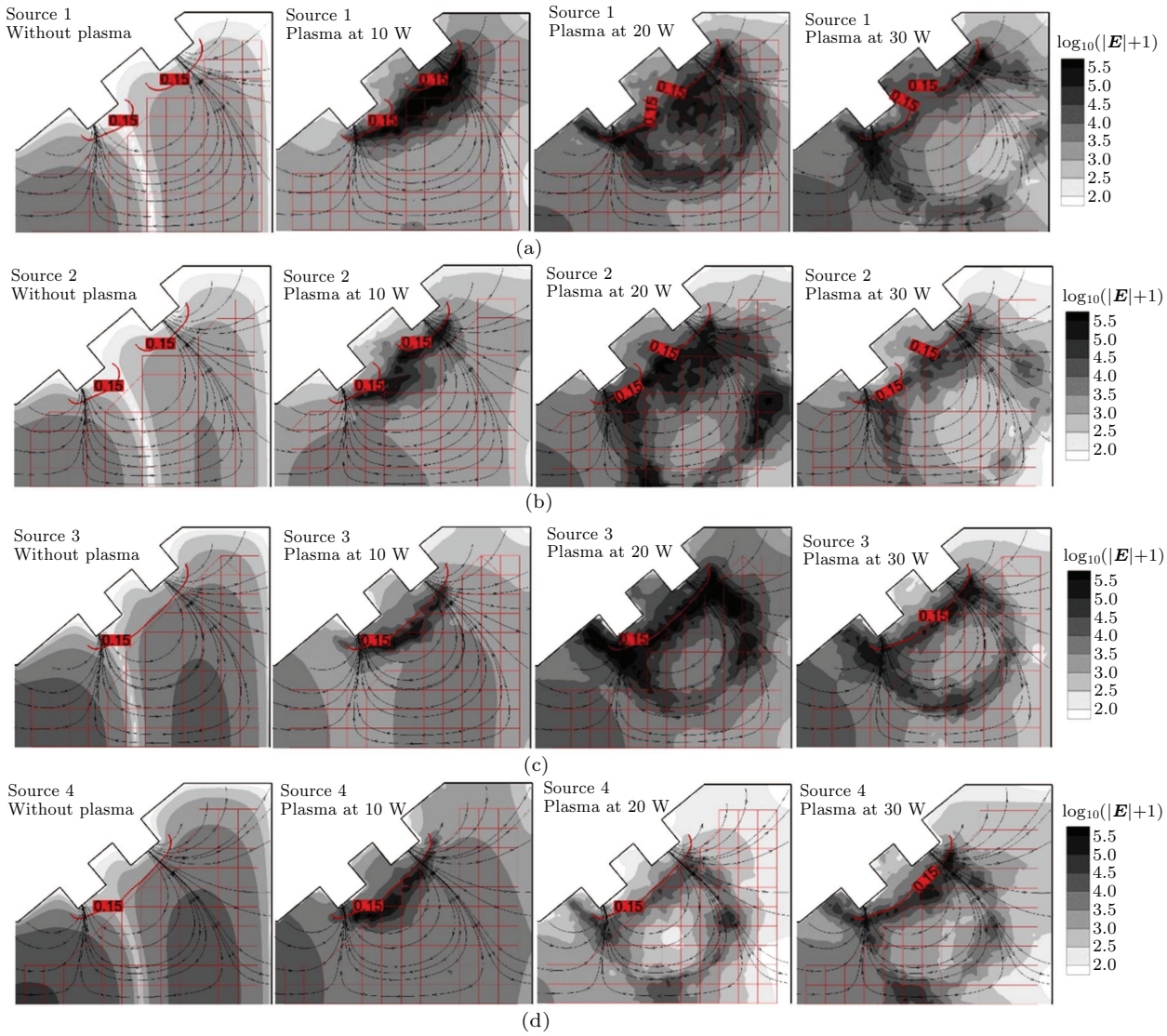


Fig. 6. Calculated parameter in source (a) 1, (b) 2, (c) 3, (b) 4 separately with plasma generated at power of 0, 10 W, 20 W and 30 W.

3.3. The revelation obtained from study

For ion thruster with gas propellant, the thrust can be calculated by[24]

$$T = \gamma I_{\mathrm{b}} \sqrt{\frac{2MV_{\mathrm{b}}}{e}}, \tag{6}$$

where γ, I_{b}, M, and V_{b} are the correction parameter of beam divergence angle and the divalent ion, the extracted ion beam current, ion mass and acceleration voltage, respectively. Therefore, thrust is proportional to I_{b} assuming the other parameters in constant. The extracted ion beam current is calculated by

$$I_{\mathrm{b}} = 0.61 e n_0 \left(eT_{\mathrm{e}}/M\right)^{1/2} A_{\mathrm{s}} T_{\mathrm{s}}, \tag{7}$$

where A_{s}, T_{s}, n_0 and T_{e} are grid area, ion transmittance of screen grid, electron density at the sheath boundary upstream of the screen grid, and electron temperature, respectively. The two relations show that the high and uniform distribution of plasma density upwind the screen grid is a critical factor to generate high thrust and ion beam current.

The ion beam extracting experiment data in Ref. [9] is showed by Table 2, in which the data is coincide with the plasma diagnosing result. It can be seen from the table, for source 1 at power of 30 W, the ion beam current is the highest. It satisfies the relation (7), because the above study of source 1 operating at 30 W present the highest density distribution and the bow formed by calculated parameter value are all nearest

to the screen grid. At the power of 10 W and 20 W, the ion beam currents from source 2 are the highest, which is consistent with that the highest density distribution and calculated bow shape are nearest to the screen grid.

Table 2. Measured total ion beam current.

Source / Ion beam	Source 1			Source 2			Source 3			Source 4		
	10 W	20 W	30 W	10 W	20 W	30 W	10 W	20 W	30 W	10 W	20 W	30 W
Current (mA)	38	100	110	100	115	100	30	30	50	25	90	78

Two revelations from the diagnosing and calculation can be obtained. The first is that when creating an ECR ion source the balance between gas ionization and electron loss must been considered. The former process is related with plasma generation region 1, ECR layer and power level, and the letter procedure is associated with the electron migrating range in the region 1 and loss in region 3, both of which are decided by the magnetic field. Therefore, as the power is restricted, the trade of plasma generation and electron loss should be taken for consideration to find a best thrust performance at reasonable magnetic field structure and power level. The second is that the microwave electric field intensity, represented by the calculated parameter, is found to be tightly related with the thrust and extracted beam performance. Experiment diagnosing data provides the microwave electric field intensity calculation with more actual information, which makes the relation of plasma and microwave electromagnetic field, and ion source evaluation actually.

4. Conclusion

In the ECR ion source, the interrelationship between plasma, magnetic field and microwave electric field is studied through the diagnosing and calculation. The results show the plasma distribution is decided by plasma generation and loss procedures, both of which are related with magnetic field. The variations of plasma density and the microwave electric field intensity are contrary as microwave transmitting in plasma, from which the condition for best performance of ECR ion source can be obtained. The conclusions are as following.

(1) The diagnosed plasma density by bended probe reviews the relationship between plasma and magnetic fields. In the ion source, electrons absorb microwave energy to ionize gas according to ECR heating procedure. At different microwave power level, the action of electron heating and loss procedures on plasma generation are different. At low power, few electrons heated by ECR wave causes its loss to control the plasma density distribution. At high power condition, the action of electron heating is stronger than its loss and controls the plasma density distribution. The plasma density distribution forms bow shape, the density in the center of the shape is higher than that in the boundary region. If the plasma density upwind the grid screen is higher, the performance of ion beam extracting and thrust will be better.

(2) Based on the cold plasma hypothesis and the plasma diagnosing result, the microwave electric field intensity calculation shows that the plasma density significantly changes the wave field distribution to form bow shape. As the calculated parameter distribution inside of the bow shape varies from higher to lower, the plasma density will relatively be changed from lower to higher. If the bow and its inside lower electric field intensity region are close to the screen grid, the performance of ion beam extracting and thrust will be better.

(3) When creating an ECR ion source, the balance between gas ionization and electron loss must be considered. The two procedures are related with plasma generation region, ECR layer, power level, and electron loss decided by magnetic field. As the power is restricted, the trade of plasma generation and electron loss should be taken for consideration to find a best thrust performance. The microwave electric field intensity in plasma is found to be tightly related with the thrust and extracted ion beam performance. Experiment diagnosing data could provide microwave electric field intensity calculation with more actual information.

Data availability

The data that support the findings of this study are available from the corresponding author upon reasonable request.

Acknowledgement

Project supported by the National Natural Science Foundation of China (Grant No. 11875222).

References

[1] Funaki I, Kuninaka H and Toki K 2004 *J. Propul. Power* **20** 718
[2] Kuninaka H, Nishiyama K, Funaki I, Shimizu Y, Yamada T and Kawaguchi J 2010 *IEEE Trans. Plasma Sci.* **34** 2125
[3] Normile D 2010 *Science* **328** 565
[4] Leva D, Myers M R, Lemmer M K, Kolbeck J, Koizumi H and Polzin K 2009 *Acta Astronaut.* **159** 213
[5] Little B and Jugroot M 2019 *Vacuum* **164** 367
[6] Jackson S W and Marshall R 2018 *J. Spacecr. Rockets* **55** 632
[7] Wahlstrand J K, Cheng Y H, Chen Y H and Michberg H M 2011 *Phys. Rev. Lett.* **107** 103901
[8] Fritsche B, Chevolleau T, Kourtev J, Kolitsch A and Möller W 2003 *Vacuum* **69** 139
[9] Jin Y Z, Yang J, Feng B B, Luo L T and Tang M J 2016 *Acta Phys. Sin.* **65** 045201 (in Chinese)
[10] Coral G, Tsukizaki R, Nishiyama K and Kuninaka H 2018 *Plasma Sources Sci. Technol.* **27** 095015

[11] Tani Y, Tsukizaki R, Koda D, Nishiyama K and Kuninaka H 2019 *Acta Astronaut.* **157** 425
[12] Jin Y Z, Yang J, Tang M J, Luo L T and Feng B B 2016 *Plasma Sci. Technol.* **18** 744
[13] Celona L, Gammino S, Ciavola G, Maimone F and Mascali D 2010 *Rev. Sci. Instrum.* **81** 02A333
[14] Sado P and Fredriksen A 2020 *IEEE Trans. Plasma Sci.* **48** 4181
[15] Ise T, Tsukizaki R, Togo H, Koizumi H and Kuninaka H 2012 *Rev. Sci. Instrum.* **83** 124702
[16] Yamashita Y, Tani Y, Tsukizaki R, Koda D and Nishiyama K 2019 *Phys. Plasmas* **26** 073510
[17] Torrisi G, Mascali D, Sorbello G, Neri L, Celona L, Castro G, Isernia T and Gammino S 2014 *J. Electromagnetic Wave* **28** 1085
[18] Chen F F 1974 *Introduction to Plasma Physics* (New York: Springer US)
[19] Kato Y, Yano K, Nishiokada T, Nagaya T, Kimura D, Kumakura S, Imai Y, Hagino S, Otsuka T and Sato F 2016 *Rev. Sci. Instrum.* **87** 02A710
[20] Xia X, Yang J, Jin Y Z, Hang G R, Fu Y L and Hu Z 2020 *Vacuum* **179** 109517
[21] Yang J, Fu Y L, Liu X C, Meng H B and Jin Y Z 2018 *Plasma Sci. Technol.* **20** 085402
[22] Fu Y L, Yang J, Geng H, Wu X C, Hu Z and Xia X 2020 *Vacuum* **184** 109932
[23] Guo S H 2008 *Electrodynamics* (Beijing: Higher Education Press)
[24] Goebel D M and Katz I 2008 *Fundamentals of Electric Propulsion: Ion and Hall Thrusters* (New Jersey: John Wiley & Sons)